Scientific Journal of Impact Factor (SJIF): 5.71
e-ISSN (O): 2348-4470
p-ISSN (P): 2348-6406

International Journal of Advance Engineering and Research Development

Volume 5, Issue 04, April -2018

STUDY ON THE LOW-VOLTAGE RIDE-THROUGH PERFORMANCE OF BRUSHLESS DOUBLY FED RELUCTANCE GENERATOR UNDER SYMMETRICAL VOLTAGE DIPS

P.K.Sarkar[1], P.K.Gayen[2], D.Chatterjee[3]

[1]*Electrical Engineering Department, Government College of Engg & Textile Tech, Berhampore, India.*
[2]*Electrical Engineering Department, Kalyani Government Engineering College, Nadia, India.*
[3]*Electrical Engineering Department, Jadavpur University, Kolkata, W.B*

Abstract- *This paper presents the low-voltage ride-through (LVRT) performance of brushless doubly fed reluctance generator (BDFRG) under symmetrical voltage dips and recovery conditions. The BDFRG is found suitable alternative for generating electrical energy from wind energy. The power (primary) winding of the machine is directly connected to the three-phase local/distribution grid and control (secondary) winding is integrated to the same electrical power network through back-to-back (dual) converter. In practice, there is the possibility of sudden dip in the voltage of connected grid and the voltage recovery starts after some elapsed time. Therefore, the paper focuses on the behavior of BDFRG from voltage dip to recovery time span. The transient currents in primary winding, momentary torque pulsation and speed rise are the consequences under the abnormal condition of symmetrical voltage dips and recovery. The ride-through performances of BDFRG are studied in this paper using MATLAB-SIMULINK software.*

Keywords- *Brushless doubly fed reluctance generator (BDFRG), low-voltage ride-through (LVRT), symmetrical voltage dip, voltage recovery, torque pulsation.*

Nomenclature

v_p, v_c	Primary and secondary winding voltage respectively
i_p, i_c	Primary and secondary winding current respectively
ω_p, ω_c	Radian frequency of primary and secondary winding variables respectively
ω_{rot}	Rotational speed in rad/sec
p_p, p_c	No. of pole pairs of primary and secondary winding
p_{rot}	No. of pole pairs of rotor
T_{em}, T_m	Electromagnetic and mechanical torque
L_p, L_c	Primary and secondary winding total inductance respectively
L_{pc}	Mutual inductance
R_p, R_c	Primary and secondary winding total resistance respectively
λ_p, λ_c	Primary and secondary winding flux linkage respectively
J	Moment of inertia of rotor
$*$	Conjugate operator
$\rightarrow$	Space vector notation
BDFRG	Brushless Doubly Fed Reluctance Generator

I. Introduction

In recent years, emphasis is given on the cultivation of wind electrical energy [1]. For this purpose, synchronous generator [2] can be employed for constant speed operation at the cost of lower efficiency of the conversion system. For variable speed operation, doubly-fed induction generator (DFIG) [3] can be employed. But the cost of the DFIG is high and reliability is low due to presence of slip rings and brushes. The problem of higher cost and low reliability can be overcome by using brushless doubly fed induction generator [4]. Now a days, it has been found that brushless doubly fed reluctance generator (BDFRG) can be efficiently used in wind energy conversion system (WECS) [5]. In BDFRG concept, the stator has two three-phase windings- namely, power (primary) and control (secondary) windings and the rotor is salient pole reluctance in nature [6]. The two stator windings must have different pole numbers so that they do not magnetically coupled directly. The rotor is designed in such a way that it helps to couple the magnetic fields produced by both stator windings. The power winding is directly connected to the nearby grid and the control winding is connected to the same grid through back-to-back (dual) controlled converter. This machine has the advantage of partially rated power electronics converter. In WECS, when the generator is connected to the grid, should comply with grid code [7].

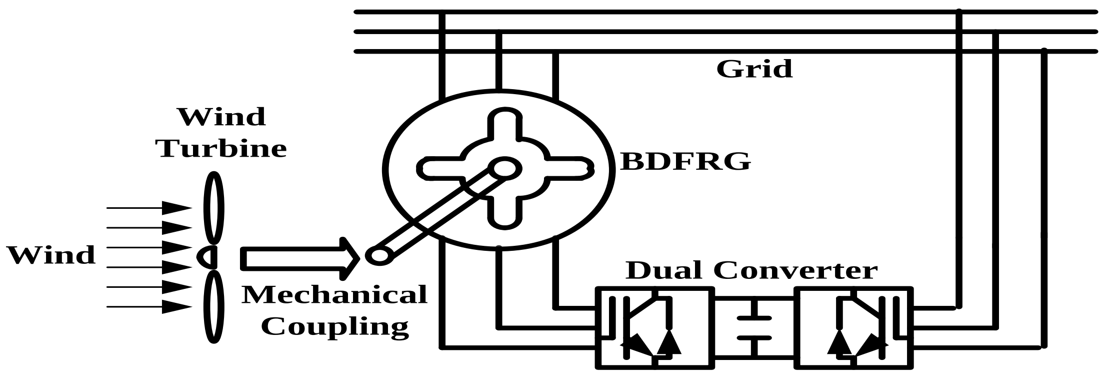

Fig. 1: Local grid connected BDFRG

The generator used in WECS, should remain connected and supply reactive power to the grid under grid voltage dips [8]. Various control strategies of BDFRG have been discussed in various published papers [9-16]. Performance of BDFRG under voltage harmonics has also been studied [17]. No significant study on low voltage ride-through (LVRT) performance [18] of BDFRG has been noticed to the best of authors' knowledge. Therefore, this paper concentrates on the study on the LVRT performance of BDFRG under symmetrical voltage dips condition. The transient current in power winding is noticed due to sudden dips in grid voltage. As a result, the active and reactive power oscillations appeared in primary winding of BDFRG. The torque oscillation and speed rise is observed under the abnormal condition of symmetrical voltage dips. This study will be helpful to design a control strategy for improving LVRT capability of grid connected BDFRG.

The dynamic modeling of BDFRG is discussed in section II. Section III describes the LVRT performance of BDFRG under symmetrical voltage dips condition. Section IV presents the results of simulation study. The paper concludes its findings in section V. The appendix and references follow section V.

II. DYNAMIC MODELING OF BDFRG

The dynamic modeling of BDFRG has been discussed in [18]. The governing equations of BDFRG are presented in the following equations in space vector form as,

$$\vec{v}_p = R_p \vec{i}_p + \frac{d\vec{\lambda}_p}{dt} \tag{1}$$

$$\vec{v}_c = R_c \vec{i}_c + \frac{d\vec{\lambda}_c}{dt} \tag{2}$$

$$\vec{\lambda}_p = L_p \vec{i}_p + L_{pc} \vec{i}_c^{\,*} \tag{3}$$

$$\vec{\lambda}_c = L_c \vec{i}_c + L_{pc} \vec{i}_p^{\,*} \tag{4}$$

The rotor speed and pole number are related to that of the primary and secondary windings as given below,

$$\omega_{rot} = \omega_p + \omega_c \tag{5}$$

$$p_{rot} = p_p + p_c \tag{6}$$

The dynamic torque-speed equation governing the rotational motion of rotor is given as,

$$T_m - T_{em} = J\frac{d\omega_{rot}}{dt} \tag{7}$$

In Eq. (7), the electromagnetic torque is mathematically expressed as,

$$T_{em} = j\frac{3}{4}p_{rot}L_{pc}[\vec{i}_p^*\vec{i}_c^* - \vec{i}_p\vec{i}_c] \tag{8}$$

The symbols used in Eq. (1)-(8) are described in the nomenclature section.
The d-q axis equations in stationary reference frame are expressed as,

$$\begin{cases} v_{pd} = R_p i_{pd} + \dfrac{d\lambda_{pd}}{dt} - \omega_p\lambda_{pq} \\ v_{pq} = R_p i_{pq} + \dfrac{d\lambda_{pq}}{dt} + \omega_p\lambda_{pd} \end{cases} \tag{9}$$

$$\begin{cases} v_{cd} = R_c i_{cd} + \dfrac{d\lambda_{cd}}{dt} - \omega_c\lambda_{cq} \\ v_{cq} = R_c i_{cq} + \dfrac{d\lambda_{cq}}{dt} + \omega_c\lambda_{cd} \end{cases} \tag{10}$$

The expressions of active and reactive power are given below,

$$P_p = i_{pd}v_{pd} + i_{pq}v_{pq} \tag{11}$$

$$Q_p = i_{pd}v_{pq} - i_{pq}v_{pd} \tag{12}$$

The d-q axis equivalent circuit diagram of BDFRG is shown in Fig. 2. Here, L_{pl}, L_{cl} denote leakage inductance of primary and secondary windings respectively. The d-q axis equivalent circuit diagram of BDFRG is shown in Fig. 2.

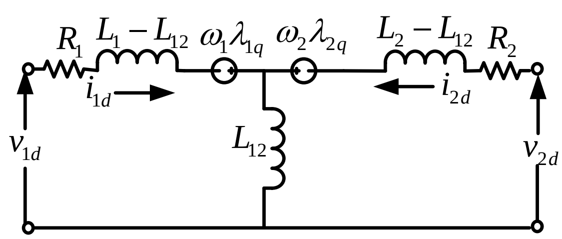

(a)

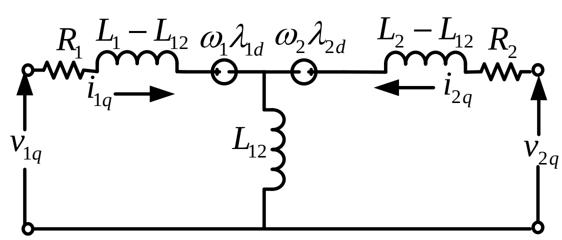

(b)

Fig. 2: (a) d-axis model, (b) q- axis model of BDFRG

The primary voltage in space vector form under normal operating condition can be written respectively as,

$$\vec{v}_p = V_p.e^{j\omega_p t} \tag{13}$$

$$\vec{v}_p = dV_p.e^{j\omega_p t} \tag{14}$$

In Eq. (14), 'd' indicates depth of voltage dip.
The resulting primary winding current consists of two components as given below,

$$\vec{i}_p = \vec{i}_{pt} + \vec{i}_{ps} \tag{15}$$

where, $\vec{i}_{pt}$, $\vec{i}_{ps}$ denotes the transient and steady state part of the primary current.
The transient and steady state part of the primary current is expressed as,

$$\vec{i}_{pt} = -\left(dV_p / R_p\right).e^{-\left(t/\tau_p\right)} \tag{16}$$

$$\vec{i}_{ps} = \left[(1-d)\left(V_p / R_p\right)\right].e^{j\omega_p t} \tag{17}$$

where, $\tau_p = L_p / R_p$.
The electromagnetic torque under voltage dips situation is mathematically represented as,

$$T_{em} = \begin{cases} j\dfrac{3}{4} p_{rot} L_{pc} [\left(\vec{i}_{pt} + \vec{i}_{ps}\right)^* \left(\vec{i}_{ct} + \vec{i}_{cs}\right)^* \\ -\left(\vec{i}_{pt} + \vec{i}_{ps}\right)\left(\vec{i}_{ct} + \vec{i}_{cs}\right)] \end{cases} \tag{18}$$

IV. Results

The MATLAB-SIMULINK software is used to develop the model of three-phase grid connected BDFRG for studying the LVRT performance of BDFRG under symmetrical voltage dips situation. The specifications of the BDFRG are provided in Appendix. In this simulation study, the model is run for total simulation time span of 15 sec in SIMULINK platform. The voltage dips starts at simulation time 't' = 6 sec. Tn this study, the voltage dip depth 'd' is taken as 0.6 p.u.. After that, the voltage recovery starts at t = 6.5 sec. The primary winding voltage recovers to its normal value at time t= 7 sec. The profile of a-phase primary winding voltage is shown in Fig. 3.

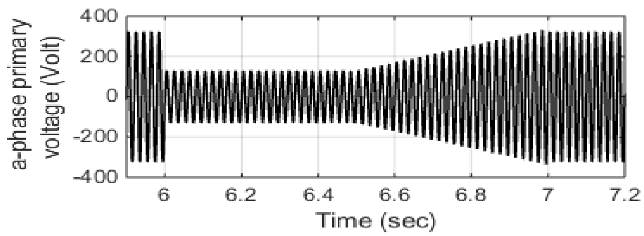

Fig.3: a-phase primary voltage waveform

The a-phase secondary winding voltage in the study is shown in Fig. 4.

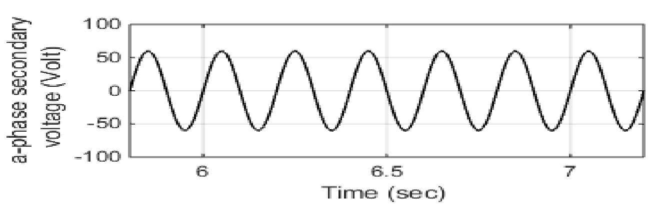

Fig.4: a-phase secondary winding voltage waveform

The current waveforms of primary and secondary windings in the study are presented in Fig. 5. Fig. 5 shows that the primary current transient decays and settles to steady state value during voltage dips. During recovery period, the primary current ramps up to the normal value.

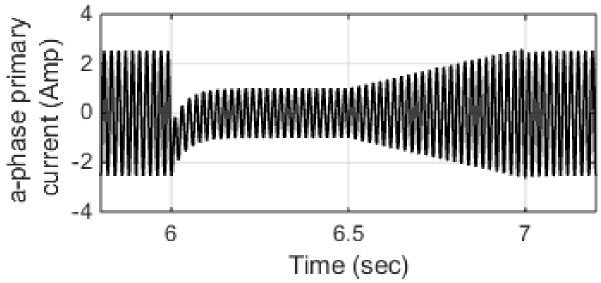

(a)

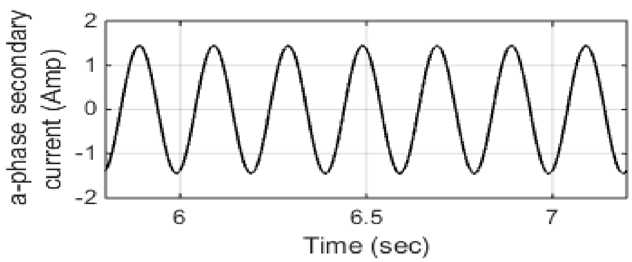

(b)

Fig.5: a-phase current in (a) primary and (b) secondary windings

The obtained active and reactive power at primary winding is shown in Fig. 6.

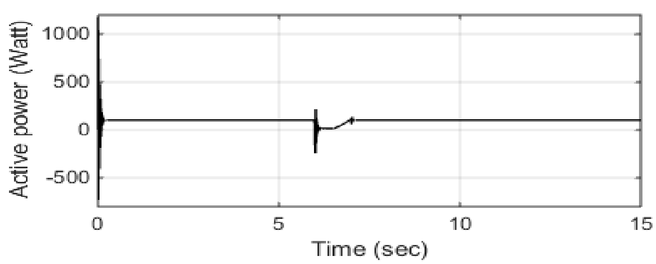

(a)

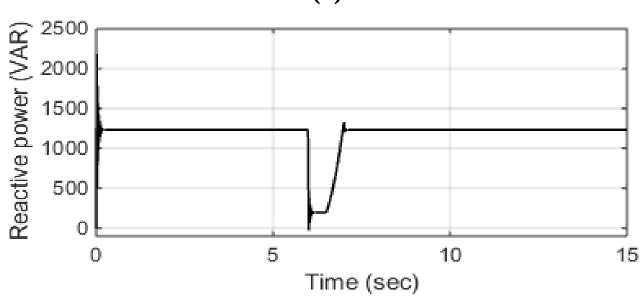

(b)

Fig.6: Three-phase (a) active and (b) reactive power at primary winding

The corresponding d-axis and q-axis primary winding fluxes are shown in Fig. 7. The obtained torque and speed responses during normal, voltage dips and recovery are represented in Fig. 8. The input mechanical torque is presented in Fig. 9.

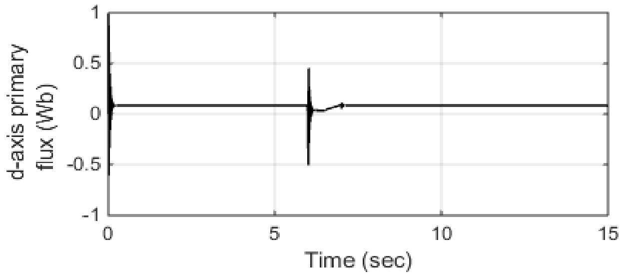

(a)

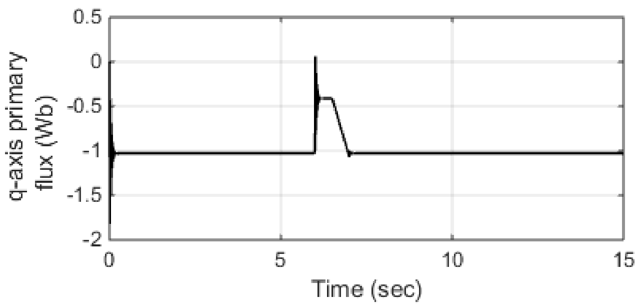

(b)

Fig.7: (a) d-axis and (b) q-axis primary winding flux.

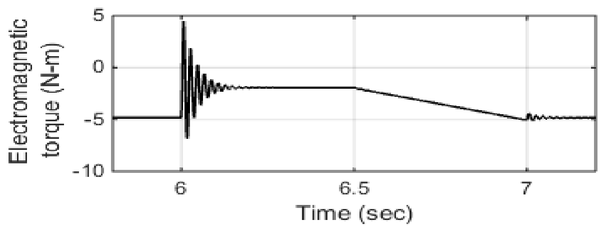

(a)

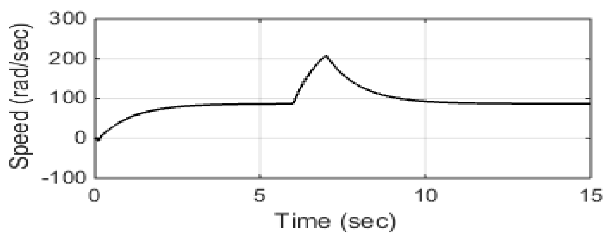

Fig.8: (a) Electromagnetic torque and (b) rotor speed

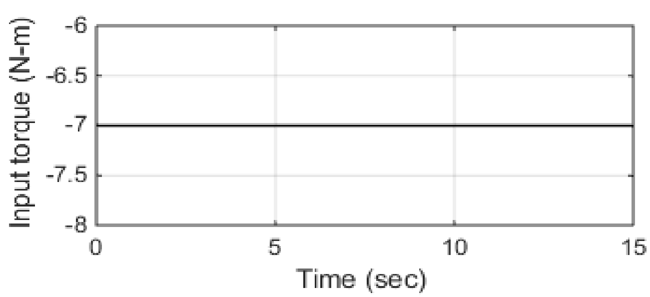

Fig.9: Input mechanical torque

V. CONCLUSION

This paper studies on the low-voltage ride-through performance of three-phase grid connected BDFRG under symmetrical grid voltage dips. The sudden voltage dips in primary winding create transient current in this winding. The peak value of the transient current is not high like the case DFIG which is widely used in WECS. The flux in the primary winding of BDFRG is of decaying oscillatory in nature after voltage dips. The significant amount of pulsation in electromagnetic torque is also noticed in the study. The rise in speed indicates the increment of stored energy into the rotor of the machine. The active power pulsation and reduction of reactive power in the primary winding are also two important consequences under symmetrical voltage dips condition. This study will be helpful to frame suitable LVRT control strategy for BDFRG to mitigate or reduce the undesired behavior of BDFRG in the abnormal condition.

Appendix

TABLE I
SPECIFICATIONS OF BDFRG

PARAMETERS	VALUES
Power	1.5 kW
Voltage	415 V
R_p, L_p	10.7 Ω, 0.407 H
R_c, L_c	12.68 Ω, 1.256 H
L_{pc}	0.57 H
J	0.1 kg/m^2
p_p, p_c, p_{rot}	6,2,4

REFERENCES

[1] M. Glinkowski, J. Hou, and G. Rackliffe, “Advances in wind energy technologies in the context of smart grid,” *Proc. IEEE*, vol. 99, no. 6,pp. 1083-1097, Jun. 2011.
[2] M. Cheah-Mane, J. Liang, and N. Jenkins, “Permanent magnet synchronous generator for wind turbines: Modelling, control and inertial frequency response,” in *Proc. 49th Int. Univ. Power Eng. Conf.*, Sep.2014, pp. 1-6.
[3] S. Muller, M. Deicke, and R. W. De Doncker, “Doubly fed induction generator systems for wind turbines,” *IEEE Ind. Appl. Mag.*, vol. 8, no. 3,pp. 26-33, May/Jun. 2002.
[4] T. Logan, J. Warrington, S. Shao, and R. McMahon, “Practical deployment of the Brushless Doubly-Fed Machine in a medium scale wind turbine,” *2009 International Conference on Power Electronics and Drive Systems (PEDS)*, pp. 470-475, Nov. 2009.
[5] M. G. Jovanović, R. E. Betz, and J. Yu, “The use of doubly fed reluctance machines for large pumps and wind turbines,” *IEEE Trans. Ind. Appl.*, vol. 38, no. 6, pp. 1508–1516, Nov./Dec. 2002.
[6] A. Knight, R. Betz, and D. Dorrell, “Design and analysis of brushless doubly fed reluctance machines,” *IEEE Trans. Ind. Appl.*, vol. 49, no. 1,pp. 50–58, Jan./Feb. 2013.
[7] R. Piwko, N. Miller, R. Girad, J. MacDowell, and K. Clark, “Generator fault tolerance and grid codes,” *IEEE Power Energy Mag.*, vol. 8, no. 2, pp. 18-26, Mar. 2010.
[8] Y. Zhang, Z. Duan, and X. Liu, “Comparison of grid code requirements with wind turbine in china and europe,” in *Proc. Asia-Pacific Power Energ.Eng. Conf.*, 2010, pp. 1-4.
[9] R. E. Betz and M. G. Jovanović, “Theoretical analysis of control properties for the brushless doubly fed reluctance machine,” *IEEE Trans. Energy Convers.*, vol. 17, no. 3, pp. 332-339, Sep. 2002.
[10] M. Jovanovic, “Sensored and sensorless speed control methods for brushless doubly fed reluctance motors,” *IET Elect. Power Appl.*, vol. 3, no. 6,pp. 503–513, 2009.
[11] S.Ademi and M. G. Jovanović, “Vector Control Methods for Brushless Doubly Fed Reluctance Machines,” *IEEE Trans. Ind. Electron.*, vol. 62, no. 1, pp. 96-104, Jan. 2015.

[12] L. Xu, L. Zhen, and E. Kim, "Field-orientation control of a doubly excited brushless reluctance machine," *IEEE Trans. Ind. Appl.*, vol. 34, no. 1, pp. 148-155, Jan./Feb. 1998.

[13] M. G. Jovanović, J. Yu, and E. Levi, "Encoderless direct torque controller for limited speed range applications of brushless doubly fed reluctance motors," *IEEE Trans. Ind. Appl.*, vol. 42, no. 3, pp. 712-722, May/Jun. 2006.

[14] H. Chaal and M. G. Jovanović, "Power control of brushless doubly-fed reluctance drive and generator systems," *Renew. Energy*, vol. 37, no. 1,pp. 419-425, 2012.

[15] H. Chaal and M. G. Jovanović, "Toward a generic torque and reactive power controller for doubly fed machines," *IEEE Trans. Power Electron.*, vol.27, no. 1, pp. 113-121, Jan. 2012.

[16] H. Chaal and M. G. Jovanović, "Practical implementation of sensorless torque and reactive power control of doubly fed machines," *IEEE Trans. Ind. Electron.*, vol. 59, no. 6, pp. 2645-2653, Jun. 2012.

[17] P.K. Sarkar, P.K. Gayen, 'Study on the Performance of Brushless Doubly Fed Reluctance Generator under Voltage Harmonics," IJARSE, vol. no-07, Special issue no-04, page no-378-387

[18] T. Long, S. Shao, E. Abdi, P. Malliband, M. E. Mathekga, R. A. Mcmahon, and P. J. Tavner, "Symmetrical low voltage ride-through of a 250 kw brushless dfig under a symmetrical full voltage dip," in *Proc. 6th IET Int. Conf. Power Electron. Mach. Drives*, Mar. 2012, pp. 1-6.

